RSC Advances

PAPER

View Article Online
View Journal | View Issue

Cite this: *RSC Adv.*, 2023, **13**, 36293

Intermolecular *exo*-selective Diels–Alder reaction catalysed by dual-functional Brønsted acid: conformational restriction of transition states by hydrogen bonds as the key interaction†

Taishi Nakanishi and Masahiro Terada *

An *exo*-selective Diels–Alder (*exo*-DA) reaction in which the formed diastereomer is different from that formed in the conventional *endo*-selective Diels–Alder (*endo*-DA) reaction was developed, which involves a dual-functional Brønsted acid as a catalyst and not only a dienophile (vinylquinoline) but also an acyclic diene (dienylcarbamate) having a sterically less demanding substituent. Factors necessary for achieving the *exo*-DA reaction were extracted through an exhaustive computational search of the corresponding transition states, in which the relative orientation of the dienophile and the acyclic diene is firmly defined by hydrogen bonding interactions with a dual-functional Brønsted acid catalyst. It was experimentally verified that the combined use of the dual-functional acid catalyst, such as phosphoric acid, and the conformationally restricted diene (dienylcarbamate), which was realized by the introduction of a substituent at the 2-position of the diene unit, is the key to achieving the *exo*-DA reaction. A catalytic enantioselective *exo*-DA reaction was also attempted by using a chiral phosphoric acid catalyst, which gave rise to the corresponding *exo*-adduct with fairly good enantioselectivity.

Received 10th November 2023
Accepted 4th December 2023

DOI: 10.1039/d3ra07688a

rsc.li/rsc-advances

Introduction

The Diels–Alder (DA) reaction is one of the most fundamental and versatile reactions for the synthesis of six-membered cyclic compounds and is widely used in total synthesis and other applications, whether in an intra- or intermolecular fashion (Fig. 1).[1] In general, intermolecular normal-electron-demand DA reactions proceed in an *endo*-selective manner.[2,3] The secondary orbital interaction has long been considered a major contributing factor to the *endo* selectivity, although dipoles, magnetic properties, and steric effects have also been found to play an important role; this issue is still being actively debated.[4] On the other hand, the development of the *exo*-selective DA (*exo*-DA) reaction, in which the formed diastereomer is different from that formed by the conventional *endo*-selective DA (*endo*-DA) reaction, is an uphill battle for synthetic organic chemists, and considerable effort has been devoted to its development because the comprehensive synthesis of stereoisomers is achieved using versatile DA reactions.

exo-DA reactions are generally achieved by using bulky catalysts or bulky dienes and dienophiles to restrict the directions of approach of these components in the transition state (TS), in which the *endo*-TS is destabilized by steric repulsion, resulting in a kinetically unfavourable pathway. In principle, dienes bearing either a cyclic structure[5] or a bulky substituent[6–8] are often used. The *exo*-DA reactions have also been established by designing dienophiles including (i) dienophiles anchored in the s-*cis* conformation,[4a,9] (ii) bulky organometallic dienophiles (and dienes),[10] and (iii) acrolein derivatives having substituents at the α-position.[11] Other *exo*-selective methods originating from the use of sterically bulky Lewis acid catalysts[12] and supramolecular catalysts[13] have also been reported. However, these prior examples are essentially limited to reactions of cyclopentadiene because the use of cyclopentadiene tends to facilitate the *exo*-selective reaction. In contrast, the *exo*-DA reaction using acyclic dienes is largely unexplored, and there are only a few examples of *exo*-DA reactions achieved by using acyclic dienes, which proceed through weak non-covalent interactions, such as hydrogen bonding, rather than the steric repulsion.[14–17]

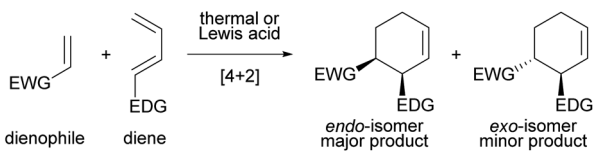

Fig. 1 Intermolecular normal-electron-demand Diels–Alder reaction, giving *endo*-isomer as the major product.

Department of Chemistry, Graduate School of Science, Tohoku University, Aramaki, Aoba-ku, Sendai, Miyagi 980-8578, Japan. E-mail: mterada@tohoku.ac.jp

† Electronic supplementary information (ESI) available. See DOI: https://doi.org/10.1039/d3ra07688a

In the *exo*-DA reaction catalysed by bulky $B(C_6F_5)_3$,[14a] detailed mechanistic studies have revealed that specific C–H···F interactions are the key to stabilizing the TS structure in the *exo*-reaction pathway.[14b] Recently, computational studies predicted an *exo*-DA reaction when the directions of approach of a diene and a dienophile were restricted by hydrogen bonding interactions,[15] although it has yet to be proven experimentally. In 1998, Wilson *et al.* reported an asymmetric *exo*-DA reaction that uses an antibody as a catalyst.[16] The DA reaction proceeded in an *exo*-selective manner without taking advantage of the steric effect of the substrates themselves. In this particular catalytic system, the relative orientation of the diene and the dienophile was controlled by the multiple hydrogen bonding interactions between the antibody catalyst and the substrates. However, the hydrogen bonding interaction approach has several limitations compared with the controlling method based on the steric repulsive effect.

Brønsted acids such as phosphoric acid and carboxylic acid are expected to exhibit dual function even though they are monofunctional acid catalysts because these molecules have both acidic and basic sites in the sole functional unit. Indeed, the dual-functional phosphoric acid unit has been effectively utilized in catalytic enantioselective reactions[18] in which a nucleophile and an electrophile are easily captured owing to the dual-functional nature of the acid catalyst through hydrogen bonding interactions, and hence the reaction proceeds in an enantioselective manner under a chiral environment created by a chiral phosphoric acid catalyst. In this context, we hypothesized that if the relative orientation of the diene and the dienophile in TSs of the DA reaction could be restricted by the hydrogen bonds formed between the dual-functional acid catalyst[19] and these substrates, the *exo*-DA reaction would be realized without having to use a bulky catalyst or the introduction of sterically demanding substituents to the substrates (Fig. 2).

To verify this hypothesis, we devised a model reaction, that is, the DA reaction of vinylquinolines **1** with dienylcarbamates **2** catalysed by phosphoric acid, which we had previously reported as an *endo*-selective reaction.[20] Computational analysis of this reaction revealed that the dual-functional nature of the phosphoric acid catalyst strictly restricts the relative orientation of the diene and the dienophile. Extraction of factors necessary for the *exo*-selectivity from this reaction system by computational studies and their experimental verification are expected to offer new insights into the control of the *endo*-/*exo*-selectivity in the DA reactions. Indeed, we developed an *exo*-DA reaction by designing the substrates and the catalytic system based on an exhaustive search for TSs using DFT calculations (Scheme 1). Herein we report new knowledge to realizing the *exo*-DA reaction, that is, not only regulating the conformational flexibility of the diene but also employing the dual-functional acid catalyst to restrict the relative orientation of the diene and the dienophile by virtue of the hydrogen bonding interaction.

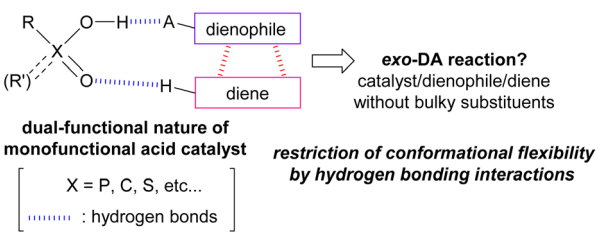

Fig. 2 Working hypothesis.

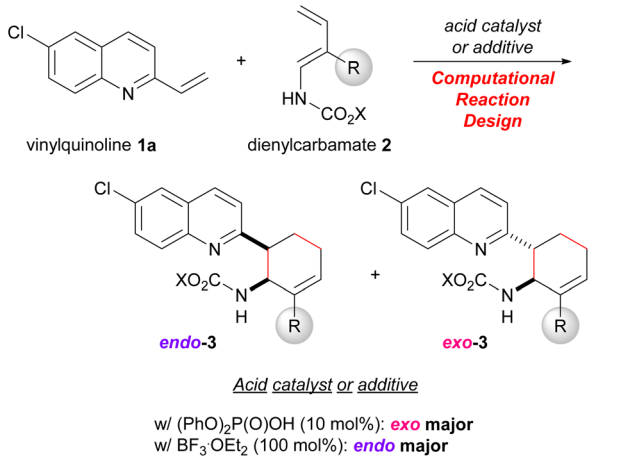

Scheme 1 The developed *exo*-DA reaction that uses a dual-functional acid catalyst.

Results and discussion

Initially, model calculations were performed to construct an evaluation system for *endo*-/*exo*-selectivity. The calculations were conducted in the gas phase at B3LYP-D3/6-31g(d) level of theory.‡[21,22] In the model calculations, vinylquinoline **1b** and dienylcarbamate **2a** were employed and all possible conformations, relative orientations, and enantiotopic faces of these substrates were considered because of using chiral phosphoric acid (*R*)-**4** as the model catalyst (Fig. 3). For vinylquinoline **1b**, there are two types of conformational isomers, s-*trans* and s-*cis*. For dienylcarbamate **2a**, four types of conformational isomers s-*cis*–*cis*, s-*cis*–*trans*, s-*trans*–*cis*, and s-*trans*–*trans*, in which the first and second s-*cis*/s-*trans* indicate the geometry of C^1–N^1–C^2–C^3 and O^1–C^1–N^1–C^2 respectively, were considered. In addition, four types of TSs, *R*-*endo*, *S*-*endo*, *R*-*exo*, and *S*-*exo*, originating from the relative orientation (*endo* and *exo*) and the enantiotopic faces (*R* and *S*) of dienylcarbamate **2a**, were generated. Totally, the existence of $2 \times 4 \times 4 = 32$ TS structures was assumed.

The calculated TSs and the relative free energies $\Delta\Delta G^{\ddagger}$ of these TSs are summarized in Table 1. All TSs of the model system indicate that the relative free energies $\Delta\Delta G^{\ddagger}$ of *R*-*endo*

‡ Since the highest priority was to grasp the overall feature of the *endo*-/*exo*-selectivity of the present DA reaction, we selected B3LYP-D3, which has a relatively low computational load. In our previous work, we thoroughly searched several functions of the DFT calculation and confirmed that B3LYP-D3 is one of the reliable ones for the transition state analysis in the present reaction system (see, ref. 20).

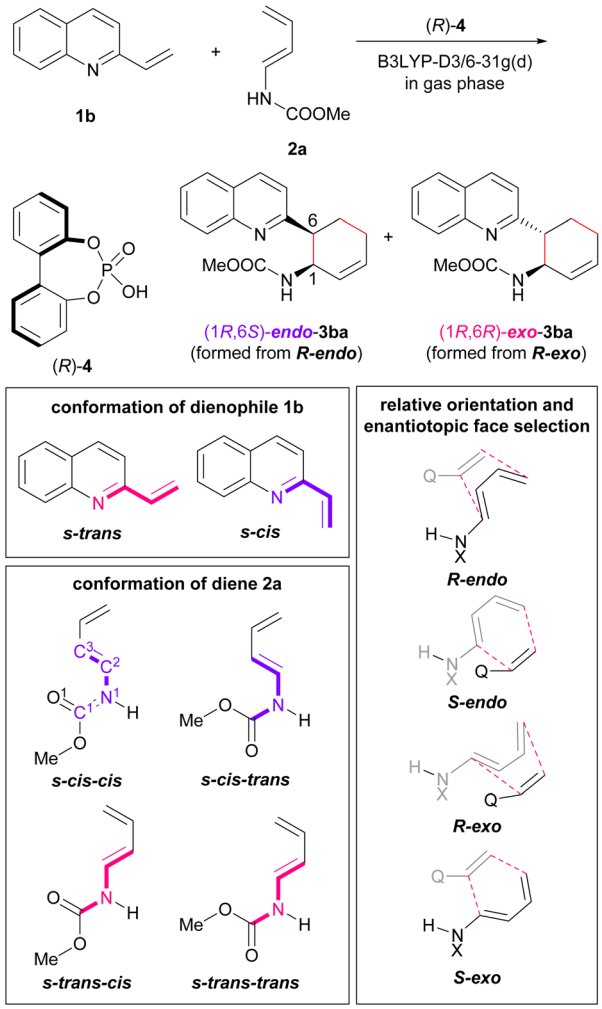

Fig. 3 Method for model calculation.

and *R-exo* TSs are comparable to those of the corresponding *S-endo* and *S-exo* TSs. Because vinylquinoline **1b** is activated through protonation at the nitrogen atom by phosphoric acid, an N–H···O hydrogen bond is formed in all TSs (Fig. 4; see ESI† for 3D structures of all TSs). Focusing on the relationship between the conformation of vinylquinoline **1b** and the free energy of TSs, overall, the s-*trans* conformation of vinylquinoline **1b** is more energetically favourable than the s-*cis* conformation. As expected, the basic site, namely, the phosphoryl oxygen, of the acid catalyst captures the dienylcarbamate through the hydrogen bond formed with the carbamate N–H proton, and hence, TSs are stabilized by this hydrogen bonding interaction. In contrast, when the carbamate N–H proton is structurally unable to interact with the phosphoryl oxygen of the catalyst, TSs are markedly destabilized. Indeed, when vinylquinoline **1b** formed the s-*cis* conformation, most of the corresponding TSs did not form a hydrogen bond and thus were unstable (see ESI† for 3D structures). At the most stable TS in the model calculation, a small difference in free energy ($\Delta\Delta G^{\ddagger}$ = 0.4 kcal mol^{-1}) was observed between *endo*-TS [**TS-Cc(R-en)**] and *exo*-TS [**TS-Tc(R-ex)**]. However, more importantly, *exo*-TS slightly

Table 1 Results of model calculation

1b	2a	TS[a]	$\Delta\Delta G^{\ddagger}$ [b] (kcal mol^{-1})	TS
s-*trans*	*cis–cis*	*R-endo*	**0.4 (0.5)**	**TS-Cc(R-en)**
		R-exo	13.7 (15.3)	—
	cis–trans	*R-endo*	**3.8 (4.1)**	**TS-Ct(R-en)**
		R-exo	16.5 (–)[c]	—
	trans–cis	*R-endo*	11.2 (11.7)	—
		R-exo	**0.0 (1.1)**	**TS-Tc(R-ex)**
	trans–trans	*R-endo*	9.5 (9.9)	—
		R-exo	**2.3 (3.5)**	**TS-Tt(R-ex)**
s-*cis*	*cis–cis*	*R-endo*	11.2 (14.3)	—
		R-exo	8.5 (7.5)	—
	cis–trans	*R-endo*	9.1 (11.6)	—
		R-exo	10.9 (10.2)	—
	trans–cis	*R-endo*	5.7 (5.6)	—
		R-exo	12.4 (11.0)	—
	trans–trans	*R-endo*	10.3 (10.9)	—
		R-exo	9.4 (7.3)	—

[a] Transition states originate from the relative orientations (*endo* and *exo*), and enantiotopic faces (*R* and *S*) are generated. [b] Relative free energies of *R-endo* and *R-exo* TSs are tabulated, and the corresponding relative free energies of *S-endo* and *S-exo* TSs are shown in parentheses. [c] The corresponding *S-exo* TS could not be optimized.

predominated despite the fact that the DA reaction generally proceeds in an *endo*-selective manner. It is considered that this small energy gap originated from the hydrogen bonding interaction between the phosphoric acid and both substrates, as shown in Fig. 4.

Furthermore, among the *R-endo* and *R-exo* TSs calculated, it was found that the four TSs are relatively stable, their energies being within 5.0 kcal mol^{-1} from the energy of the most stable TS [**TS-Tc(R-ex)**] (Table 1 and Fig. 4). Detailed analysis of these four TSs revealed that the geometry around C^1–N^1–C^2–C^3 of dienylcarbamate **2a** was different between the *endo*- and *exo*-TSs: dienylcarbamate **2a** had an s-*cis* conformation in the *endo*-TS (Fig. 4a and c) and, in contrast, an s-*trans* conformation in the *exo*-TS (Fig. 4b and d). These results suggest that if the s-*cis* conformation of dienylcarbamate is selectively destabilized, the reaction will proceed preferentially from the s-*trans* conformation, giving rise to the *exo*-adduct in a stereoselective manner. In order to establish the *exo*-DA reaction, we proposed a molecular design in which a substituent is introduced at the 2-position of the diene unit (in the previous original numbering: C^3) to destabilize the s-*cis* conformation selectively with little detrimental effect on the s-*trans* conformation (Fig. 5). On the basis of this proposal, we designed six dienylcarbamates **2b–g** having a substituent at the 2-position and calculated the difference in free energy between *endo*- and *exo*-TS in the model system. All newly designed substrates **2b–g** except **2f** (R = $SiMe_3$) were modified without having to introduce sterically demanding substituents.

DFT calculations were performed using newly designed dienylcarbamates **2b–g** having a substituent at the 2-position, vinylquinoline **1b**, and phosphoric acid (*R*)-**4**. The relative free energies of selected substrates **2b**, **2c**, and **2g** are summarized in Table 2 (all TS energies of the model system using substrates **2b–g** including *S-endo* and *S-exo* TSs are shown in ESI†). It

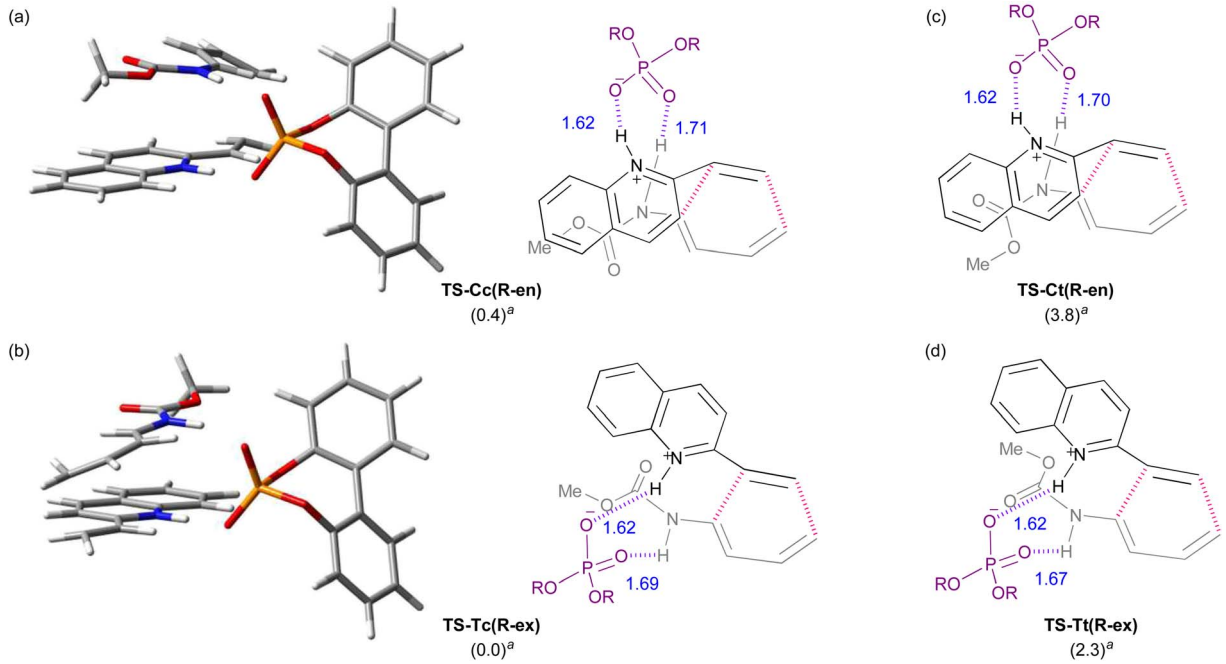

Fig. 4 3D structures and schematic models of the most stable *endo*- and *exo*-TSs: (a) *endo*-TS: **TS-Cc(R-en)**. (b) *exo*-TS: **TS-Tc(R-ex)**. Schematic models of the second most stable *endo*- and *exo*-TSs: (c) *endo*-TS: **TS-Ct(R-en)**. (d) *exo*-TS: **TS-Tt(R-ex)**. [a]Relative free energy (kcal mol^{-1}).

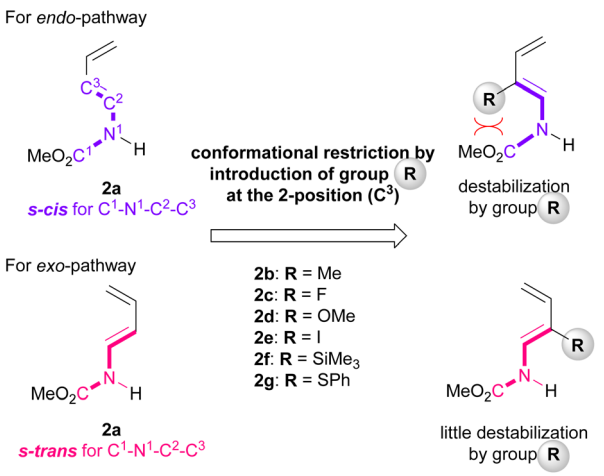

Fig. 5 Concept of newly designed substrates for *exo*-DA reaction.

became clear from the selected examples that while certain reactions through the *S*-enantiotopic face of dienylcarbamate **2** (*S-endo*) and its corresponding *R*-counterpart gave similar $\Delta\Delta G^{\ddagger}$ values, the majority of cases showed that the reaction through the *R*-enantiotopic face had a smaller $\Delta\Delta G^{\ddagger}$ value than the reaction through its *S*-counterpart. More importantly, as shown in Table 2 and all TSs in ESI,† the TSs giving the *exo*-adduct, namely, **TS_R-Tc(R-ex)** (**TS_R**: R = substituent introduced at the 2-position), are the most energetically favourable for newly designed dienylcarbamates **2b–g**. Noteworthy is the fact that dienylcarbamate **2c** having a small substituent such as fluorine at the 2-position undergoes the *exo*-DA reaction in a highly selective manner (calculated *exo*/*endo* = >20/1).

The 3D TSs and the schematic models derived from the calculations using dienylcarbamate **2b** (R = Me) are shown as a representative (Fig. 6). In the *endo*-TS, the introduction of the R group at the 2-position (in the previous original numbering: C^3) resulted in a marked steric repulsion between substituent R and the carbamate unit because C^1–N^1–C^2–C^3 of dienylcarbamate **2b** took an s-*cis* conformation. As predicted, this steric congestion resulted in a twisted conformation of the dienylcarbamates, in which the carbamate unit markedly deviated from the coplanarity with the diene unit by around 30°

Table 2 Selected examples of DFT calculations for transition states in the reaction of newly designed dienylcarbamates **2** with vinylquinoline **1b** catalysed by phosphoric acid (*R*)-**4**

R	TS	$\Delta\Delta G^{\ddagger}$ [a] (kcal mol^{-1})
Me (**2b**)	**TS_{Me}-Cc(R-en)**	5.3 (5.2)[b]
	TS_{Me}-Ct(R-en)	9.4 (9.3)[c]
	TS_{Me}-Tc(R-ex)	**0.0**
	TS_{Me}-Tt(R-ex)	2.7
F (**2c**)	**TS_{F}-Cc(R-en)**	2.7 (**2.6**)[d]
	TS_{F}-Ct(R-en)	5.3
	TS_{F}-Tc(R-ex)	**0.0**
	TS_{F}-Tt(R-ex)	2.9
SPh (**2g**)	**TS_{SPh}-Cc(R-en)**	**6.4**
	TS_{SPh}-Ct(R-en)	9.5
	TS_{SPh}-Tc(R-ex)	**0.0**
	TS_{SPh}-Tt(R-ex)	2.4

[a] Relative free energies of *R-endo* and *R-exo* TSs are shown, and the corresponding relative free energies of *S-endo* and *S-exo* TSs are partially shown in parentheses. [b] $\Delta\Delta G^{\ddagger}$ for **TS_{Me}-Cc(S-en)**. [c] $\Delta\Delta G^{\ddagger}$ for **TS_{Me}-Ct(S-en)**. [d] $\Delta\Delta G^{\ddagger}$ for **TS_{F}-Cc(S-en)**.

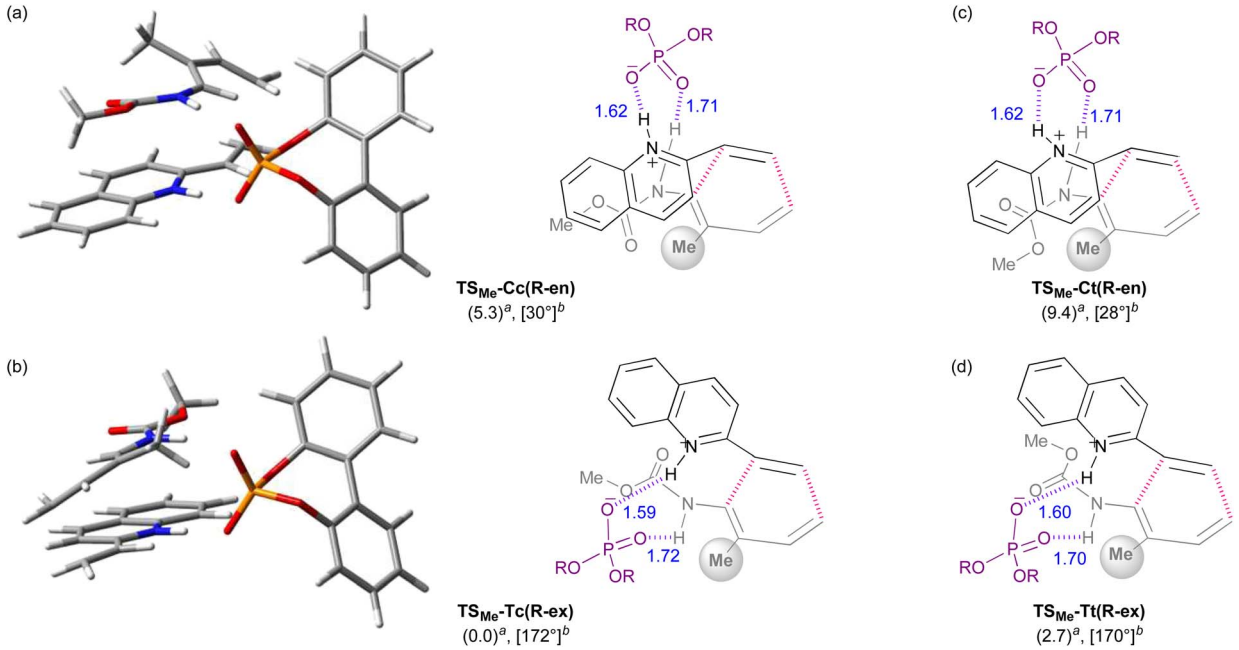

Fig. 6 DFT calculations of the transition states in the reaction of dienylcarbamate **2b** (R = Me) with vinylquinoline **1b** catalysed by phosphoric acid (*R*)-**4**. 3D structures and schematic models of the most stable *endo*- and *exo*-TSs: (a) *endo*-TS: TS$_{Me}$-**Cc(R-en)**. (b) *Exo*-TS: TS$_{Me}$-**Tc(R-ex)**. Schematic models of the second most stable *endo*- and *exo*-TSs: (c) *endo*-TS: TS$_{Me}$-**Ct(R-en)**. (d) *Exo*-TS: TS$_{Me}$-**Tt(R-ex)**. [a]Relative free energy (kcal mol^{-1}). [b]Dihedral angle of C^1–N^1–C^2–C^3 for dienylcarbamate **2b** (R = Me).

(Fig. 6a and c). In contrast, in the *exo*-TS, the introduction of the R group caused little steric repulsion because C^1–N^1–C^2–C^3 took an s-*trans* conformation (Fig. 6b and d). Hence the corresponding dihedral angle was expected to be close to 180°. Indeed, the dihedral angle was around 170° and the coplanarity between the diene and carbamate units was almost maintained. As described above, the proposal, "the introduction of substituent R at the 2-position destabilizes the s-*cis* conformation, pushing up the energy level of the *endo*-TS", was confirmed by the DFT calculations.

Our greatest concern was whether the *exo*-stereochemical outcome predicted by the DFT calculations could be verified experimentally. A newly designed substrate was investigated using dienylcarbamate **2b** having a methyl group at the 2-position (R = Me) (Table 3). Furthermore, in order to confirm the importance of the formation of hydrogen bonds between the catalyst/additive and both substrates, vinylquinoline **1a** and dienylcarbamate **2b**, we employed different acid catalyst/additive to investigate *endo*-/*exo*-selectivity in the intended DA reaction. As predicted, the use of diphenyl phosphate [$(PhO)_2P(O)OH$] as the acid catalyst facilitated the formation of an *exo*-adduct in a highly selective manner (entry 1).§ In contrast, *endo*-selectivity was predominant when the reaction was performed using Lewis acids such as boron trifluoride diethyl ether complex ($BF_3 \cdot OEt_2$)[23] and tris(pentafluorophenyl)borane [$B(C_6F_5)_3$] (entries 2 and 3). The predominant formation of the *endo*-adduct was also observed under thermal reaction conditions (without using an acid catalyst/additive) (entry 4) as a common stereochemical outcome in the intermolecular normal-electron-demand DA reaction.

§ The DA reaction of parent 2-vinylquinolines (**1b**) with **2b** using $(PhO)_2P(O)OH$ as the catalyst (condition A shown in Table 4) gave the *exo*-adduct as the major stereoisomer (69% combined yield of *endo*/*exo*-isomers) with exactly the same stereoselectivity (*endo*/*exo* = 3/97) as the DA reaction of chloro-substituted **1a** with **2b** (Table 3, entry 1).

Table 3 Investigation of catalyst/additive effect on *endo*-/*exo*-selectivity[a]

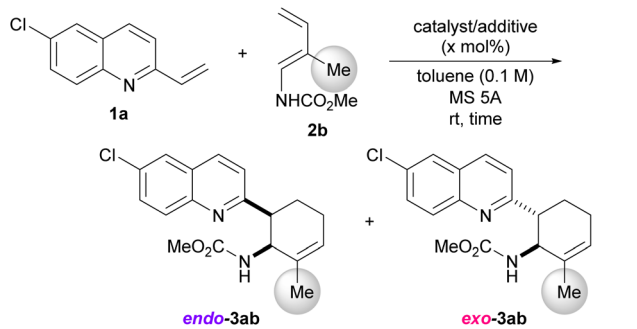

Entry	Catalyst/additive (mol%)	Time (h)	Yield[b] (%)	*Endo*/*exo*[c]
1	$(PhO)_2P(O)OH$ (10)	48	70	3/97
2[d]	$BF_3 \cdot OEt_2$ (100)	24	43	81/19
3	$B(C_6F_5)_3$ (10)	48	50	82/18
4	None, 100 °C	48	13	62/38
5	Cl_3CCO_2H (10)	48	75	15/85
6	$TsOH \cdot H_2O$ (10)	48	52	25/75

[a] Unless otherwise noted, all reactions were carried out using 0.1 mmol of **1a**, 0.12 mmol of **2b**, MS 5A (50 mg), and catalyst/additive in toluene (1 mL) at room temperature. [b] Isolated yields. [c] Determined by ^{1}H NMR measurement of the crude mixture. [d] Without MS 5A.

Table 4 Substitution patterns of dienylcarbamates and types of catalyst/additive effect on *endo*-/*exo*-selectivity[a]

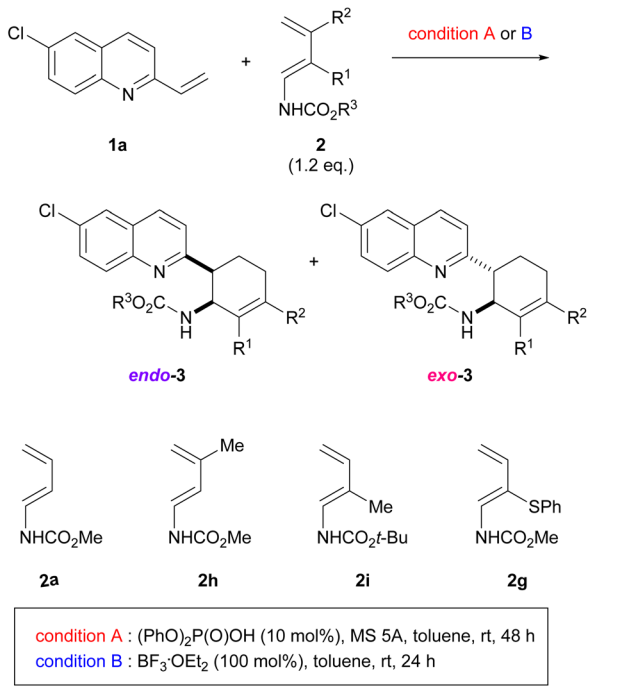

Entry	Cond.[b]	2	3	Yield[c] (%)	*Endo*/*exo*[d]
1	A	**2a**	**3aa**	68	72/28
2	B			60	83/17
3	A	**2h**	**3ah**	80	60/40
4	B			21	71/29
5	A	**2i**	**3ai**	45	25/75
6	B			50	80/20
7	A	**2g**	**3ag**	24	26/74
8	B			28	69/31

[a] Unless otherwise noted, all reactions were carried out using 0.1 mmol of **1a**, 0.12 mmol of **2**, and MS 5A (50 mg) in toluene (1 mL) at room temperature. [b] Condition A: 10 mol% $(PhO)_2P(O)OH$ was used as an acid catalyst. Condition B: 100 mol% $BF_3{\cdot}OEt_2$ was used as an acid additive. [c] Isolated yields. [d] Determined by ^1H NMR measurement of the crude mixture.

Furthermore, trichloroacetic acid and *p*-toluene sulfonic acid were considered promising candidates for the dual-functional Brønsted acid catalyst similar to phosphoric acid. In fact, under the influence of these acid catalysts, the *exo*-adduct was obtained as the major diastereomer, albeit with a slightly low selectivity (entries 5 and 6). These results indicate that the type of acid catalyst/additive has a significant impact on the *endo*-/*exo*-selectivity. As hypothesized for the present reaction system, the dual-functional nature of the acid catalyst is essential for the *exo*-DA reaction. Even if the s-*cis* conformation of dienylcarbamate is effectively destabilized by the steric effect of the substituent (R = Me in Fig. 6), no *exo*-selectivity would be achieved when no hydrogen bonds are formed between the acid catalyst and both substrates. The relative stereochemistry of **3ab** was determined by comparing the ^1H NMR coupling constants of the *endo*- and *exo*-products[7a,8b] (see ESI† for details).

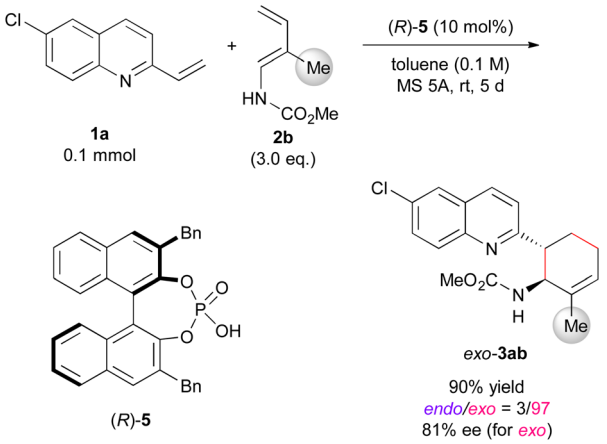

Scheme 2 Initial attempt at enantioselective *exo*-DA reaction.

Next, using a series of dienylcarbamates **2**, we investigated the substituent effect on the *endo*-/*exo*-selectivity (Table 4). In the case of simple dienylcarbamate **2a**, instead of **2b** having a methyl substituent, either diphenyl phosphate $[(PhO)_2P(O)OH]$ (condition A) or boron trifluoride diethyl ether complex $(BF_3{\cdot}OEt_2)$ (condition B) resulted in the formation of an *endo*-adduct as the major diastereomer (entries 1 and 2). Similarly, under the same reaction conditions, dienylcarbamate **2h** having a methyl group at the 3-position underwent the reaction with low to moderate *endo*-selectivity (entries 3 and 4). These results suggest that the conformational restriction of dienylcarbamate by the introduction of a substituent at the 2-position is the key to achieving an *exo*-selective reaction, as predicted by the DFT calculations (Table 2 and Fig. 5). Dienylcarbamate having a methyl substituent at the 2-position was further modified by changing the carbamate unit to the Boc group from methoxycarbonyl (entries 5 and 6). *exo*-Selectivity was observed when $(PhO)_2P(O)OH$ was used as the acid catalyst (entry 5), whereas the *endo*-adduct was produced when $BF_3{\cdot}OEt_2$ was used (entry 6). Even when the substituent at the 2-position was replaced by a thiophenyl group instead of a methyl group, $(PhO)_2P(O)OH$ facilitated the reaction in an *exo*-selective manner (entry 7). Again, the use of $BF_3{\cdot}OEt_2$ resulted in the *endo*-selectivity in the same reaction (entry 8). It should be emphasized that the combined use of the dual-functional acid catalyst and the conformationally restricted dienylcarbamate is crucial to accomplishing the DA reaction in an *exo*-selective manner.

Finally, we attempted to expand the developed *exo*-DA reaction to an enantioselective variant using chiral phosphoric acid (Scheme 2).[24] In the reaction of **1a** with **2b**, the use of (*R*)-**5** having benzyl groups at the 3,3′-positions resulted in *exo*-DA product **3ab** in good yield with high *exo*-selectivity and fairly good enantioselectivity¶ (see ESI† for catalyst screening). The number of examples of enantioselective *exo*-DA reactions using acyclic dienes under the influence of chiral catalyst[6a,7a,12j,16,25] is far fewer than those of *endo*-DA reactions. Hence, the present

¶ The absolute configuration of *exo*-**3ab** has not been determined yet.

approach provides valuable insights into the development of novel catalytic enantioselective *exo*-DA reactions using acyclic dienes.

Conclusions

We have demonstrated a novel approach to establish an *exo*-DA reaction of an acyclic diene without introducing sterically demanding substituents into either a catalyst, a dienophile (vinylquinoline), or an acyclic diene (dienylcarbamate). Factors necessary for achieving the *exo*-DA reaction, in which the relative orientation of the dienophile and the acyclic diene is firmly defined by hydrogen bonding interactions with a dual-functional Brønsted acid catalyst, were extracted by thorough computational analysis of the corresponding transition states and verified experimentally. As predicted by DFT calculations, conformational restriction of the diene (dienylcarbamate) by the introduction of a substituent at the 2-position of the diene unit is the key to achieving the DA reaction in an *exo*-selective manner. Thus, the effective utilization of the hydrogen bonding interaction realized by a combination of the dual-functional acid catalyst and the conformationally restricted diene (dienylcarbamate) is crucial to achieving the *exo*-DA reaction. The present approach is expected to give new insights into the control of *endo*-/*exo*-selectivity in the DA reactions and contribute to the development of stereodivergent methods for the DA reactions. Further studies along this line are in due course in our laboratory.

Data availability

The exploratory investigation, experimental procedures, computational data, and characterization data are available.

Author contributions

T. N. contributed conceptualization, design of the work, data curation, formal analysis, investigation (experimental and theoretical studies), and writing – original draft. M. T. contributed conceptualization, project administration, writing – review & editing, supervision, and funding acquisition.

Conflicts of interest

There are no conflicts to declare.

Acknowledgements

The computation was performed using Research Center for Computational Science, Okazaki, Japan (Project: 22-IMS-C127). This work was supported by a Grant-in-Aid for Scientific Research on Innovative Areas "Hybrid Catalysis for Enabling Molecular Synthesis on Demand" (JP17H06447) from MEXT, Japan (M. T.), a Grant-in-Aid for Challenging Research (Exploratory) (JP22K19018) from JSPS (M. T.), and a Grant-in-Aid for Young Scientists (JP21J14551) from JSPS, Japan (T. N.).

Notes and references

1 (*a*) K. C. Nicolau, S. A. Snyder, T. Montagnon and G. Vassilikogiannakis, *Angew. Chem., Int. Ed.*, 2002, **41**, 1668–1698; (*b*) M. Gregoritza and F. P. Brandl, *Eur. J. Pharm. Biopharm.*, 2015, **97**, 438–453; (*c*) M. M. Heravi, T. Ahmadi, M. Ghavidel, B. Heidari and H. Hamidi, *RSC Adv.*, 2015, **5**, 101999–102705.

2 K. Alder and G. Stein, *Angew. Chem.*, 1937, **50**, 510–519.

3 (*a*) R. Hoffmann and R. B. Woodward, *J. Am. Chem. Soc.*, 1965, **87**, 4388–4389; (*b*) R. B. Woodward and R. Hoffmann, *The Conservation of Orbital Symmetry*, Academic Press, New York, 1970.

4 (*a*) W. R. Roush and B. B. Brown, *J. Org. Chem.*, 1992, **57**, 3380–3387; (*b*) J. I. García, J. A. Mayoral and L. Salvatella, *Acc. Chem. Res.*, 2000, **33**, 658–664; (*c*) A. Arrieta, F. P. Cossío and B. Lecea, *J. Org. Chem.*, 2001, **66**, 6178–6180; (*d*) J. I. García, J. A. Mayoral and L. Salvatella, *Eur. J. Org. Chem.*, 2005, 85–90; (*e*) C. S. Wannere, A. Paul, R. Herges, K. N. Houk, H. F. Schaefer III and P. von Ragué Schleyer, *J. Comput. Chem.*, 2007, **28**, 344–361; (*f*) I. Fernandez and F. M. Bickelhaupt, *J. Comput. Chem.*, 2014, **35**, 371–376; (*g*) W. J. Lording, T. Fallon, M. S. Sherburn and M. N. Paddon-Row, *Chem. Sci.*, 2020, **11**, 11915–11926.

5 If one alkene is embedded in a congested ring structure, *exo*-selectivity is often expressed, see: (*a*) T. Yoon, S. J. Danishefsky and S. A. de Gala, *Angew. Chem., Int. Ed. Engl.*, 1994, **33**, 853–855; (*b*) J. D. Ha, C. H. Kang, K. A. Belmore and J. K. Cha, *J. Org. Chem.*, 1998, **63**, 3810–3811; (*c*) M. Ge, B. M. Stoltz and E. J. Corey, *Org. Lett.*, 2000, **2**, 1927–1929.

6 (*a*) H. Usuda, A. Kuramochi, M. Kanai and M. Shibasaki, *Org. Lett.*, 2004, **6**, 4387–4390; (*b*) G. M. Sammis, E. M. Flamme, H. Xie, D. M. Ho and E. Sorensen, *J. Am. Chem. Soc.*, 2005, **127**, 8612–8613; (*c*) Y. Zeng and J. Aube, *J. Am. Chem. Soc.*, 2005, **127**, 15712–15713.

7 (*a*) Z. Liu, X. Lin, N. Yang, Z. Su, C. Hu, P. Xiao, Y. He and Z. Song, *J. Am. Chem. Soc.*, 2016, **138**, 1877–1883; (*b*) G.-M. Ho, C.-J. Huang, E. Y.-T. Li, S.-K. Hsu, T. Wu, M. M. L. Zulueta, K. B. Wu and S.-C. Hung, *Sci. Rep.*, 2016, **6**, 35147; (*c*) J. Wang, Z. Liu, J. Li, Z. Song, C. Hu and Z. Su, *J. Org. Chem.*, 2019, **84**, 3940–3952; (*d*) C.-J. Huang and E. Y. Li, *RSC Adv.*, 2019, **9**, 7246–7250.

8 (*a*) Y.-H. Lam, C. Bobbio, I. R. Cooper and V. A. A. Gouverneur, *Angew. Chem., Int. Ed.*, 2007, **46**, 5106–5110; (*b*) Y.-H. Lam, P. H.-Y. Cheong, J. M. B. Mata, S. J. Stanway, V. Gouverneur and K. N. Houk, *J. Am. Chem. Soc.*, 2009, **131**, 1947–1957.

9 (*a*) W. R. Roush, A. P. Essenfeld, J. S. Warmus and B. B. Brown, *Tetrahedron Lett.*, 1989, **30**, 7305–7308; (*b*) K. Takeda, I. Imaoka and E. Yoshii, *Tetrahedron*, 1994, **50**, 10839–10848; (*c*) W. R. Roush, M. L. Reilly, K. Koyama and B. B. Brown, *J. Org. Chem.*, 1997, **62**, 8708–8721; (*d*) W. R. Roush and R. J. Sciotti, *J. Am. Chem. Soc.*, 1998, **120**, 7411–7419; (*e*) W. R. Roush, D. A. Barda, C. Limberakis

and R. K. Kunz, *Tetrahedron*, 2002, **58**, 6433–6454; (*f*) W. R. Roush, C. Limberakis, R. K. Kunz and D. A. Barda, *Org. Lett.*, 2002, **4**, 1543–1546; (*g*) J. Qi and W. R. Roush, *Org. Lett.*, 2006, **8**, 2795–2798.

10 (*a*) S. R. Gilbertson, X. Zhao, D. P. Dawson and K. L. Marshall, *J. Am. Chem. Soc.*, 1993, **115**, 8517–8518; (*b*) M. W. Wright, T. L. Smalley, M. E. Welker and A. L. Rheingold, *J. Am. Chem. Soc.*, 1994, **116**, 6777–6791; (*c*) B. M. Richardson and M. E. Welker, *J. Org. Chem.*, 1997, **62**, 1299–1304; (*d*) T. S. Powers, W. Jiang, J. Su, W. D. Wulff, B. E. Waltermire and A. L. Rheingold, *J. Am. Chem. Soc.*, 1997, **119**, 6438–6439; (*e*) J. Barluenga, R. M. Canteli, J. Florez, S. García-Granda, A. Gutierrez-Rodríguez and E. Martín, *J. Am. Chem. Soc.*, 1998, **120**, 2514–2522.

11 The reaction of α-substituted acrolein with cyclopentadiene is well known for its tendency to develop *exo* selectivity. see selected examples: (*a*) E. J. Corey and T. P. Loh, *J. Am. Chem. Soc.*, 1991, **113**, 8966–8967; (*b*) E. P. Kündig, B. Bourdin and G. Bernardinelli, *Angew. Chem., Int. Ed. Engl.*, 1994, **33**, 1856–1858; (*c*) Y. Hayashi, J. J. Rohde and E. J. Corey, *J. Am. Chem. Soc.*, 1996, **118**, 5502–5503; (*d*) K. Ishihara, H. Kurihara, M. Matsumoto and H. Yamamoto, *J. Am. Chem. Soc.*, 1998, **120**, 6920–6930; (*e*) Y.-C. Teo and T.-P. Loh, *Org. Lett.*, 2005, **7**, 2539–2541; (*f*) F. Fu, Y.-C. Teo and T.-P. Loh, *Org. Lett.*, 2006, **8**, 5999–6001.

12 (*a*) K. Maruoka, H. Imoto and H. Yamamoto, *J. Am. Chem. Soc.*, 1994, **116**, 12115–12116; (*b*) E. P. Kündig, C. M. Saudan, V. Alezra, F. Viton and G. Bernardinelli, *Angew. Chem., Int. Ed.*, 2001, **40**, 4481–4485; (*c*) K. Ishihara and K. Nakano, *J. Am. Chem. Soc.*, 2005, **127**, 10504–10505; (*d*) T. Kano, Y. Tanaka and K. Maruoka, *Org. Lett.*, 2006, **8**, 2687–2689; (*e*) H. Gotoh and Y. Hayashi, *Org. Lett.*, 2007, **9**, 2859–2862; (*f*) Y. Hayashi, S. Samanta, H. Gotoh and H. Ishikawa, *Angew. Chem., Int. Ed.*, 2008, **47**, 6634–6637; (*g*) M. Bakos, Z. Dobi, D. Fegyverneki, Á. Gyömöre, I. Fernández and T. Soós, *ACS Sustainable Chem. Eng.*, 2018, **6**, 10869–10875; (*h*) M. Hou, M. Xu, B. Yang, H. He and S. Gao, *Org. Lett.*, 2021, **23**, 7487–7491; (*i*) B. P. Bondzić, K. Daskalakis, T. Taniguchi, K. Monde and Y. Hayashi, *Org. Lett.*, 2022, **24**, 7455–7460; (*j*) Y.-H. Li, S.-L. Zhang, Y. Lu, B. Xiao, T.-Y. Sun, Q.-Q. Xu, J.-H. Chen and Z. Yang, *Angew. Chem., Int. Ed.*, 2023, **62**, e202303075.

13 (*a*) A. Sakakura, K. Suzuki and K. Ishihara, *Adv. Synth. Catal.*, 2006, **348**, 2457–2465; (*b*) M. Hatano, T. Mizuno, A. Izumiseki, R. Usami, T. Asai, M. Akakura and K. Ishihara, *Angew. Chem., Int. Ed.*, 2011, **50**, 12189–12192; (*c*) M. Hatano and K. Ishihara, *Chem. Commun.*, 2012, **48**, 4273–4283; (*d*) K. Matsui, K. Toh, M. Hatano and K. Ishihara, *Org. Lett.*, 2022, **24**, 6483–6488.

14 (*a*) J.-H. Zhou, B. Jiang, F.-F. Meng, Y.-H. Xu and T.-P. Loh, *Org. Lett.*, 2015, **17**, 4432–4435; (*b*) D. Yepes, P. Pérez, P. Jaque and I. Fernández, *Org. Chem. Front.*, 2017, **4**, 1390–1399.

15 D. Taherinia, M. M. Mahmoodi and A. Fattahi, *New J. Chem.*, 2021, **45**, 16760–16772.

16 A. Heine, E. A. Stura, J. T. Yli-Kauhaluoma, C. Gao, Q. Deng, B. R. Beno, K. N. Houk, K. D. Janda and I. A. Wilson, *Science*, 1998, **279**, 1934–1940.

17 D. Taherinia and A. Fattahi, *Sci. Rep.*, 2022, **12**, 22225.

18 (*a*) Y. Toda, T. Korenaga, R. Obayashi, J. Kikuchi and M. Terada, *Chem. Sci.*, 2021, **12**, 10306–10312; (*b*) J. P. Reid and J. M. Goodman, *J. Am. Chem. Soc.*, 2016, **138**, 7910–7917; (*c*) P. A. Champagne and K. N. Houk, *J. Am. Chem. Soc.*, 2016, **138**, 12356–12359; (*d*) C. Liu, M. Besora and F. Maseras, *Chem. –Asian J.*, 2016, **11**, 411–416; (*e*) F. Li, T. Korenaga, T. Nakanishi, J. Kikuchi and M. Terada, *J. Am. Chem. Soc.*, 2018, **140**, 2629–2642; (*f*) K. Kanomata, Y. Nagasawa, M. Yamanaka, Y. Shibata, F. Egawa, J. Kikuchi and M. Terada, *Chem.–Eur. J.*, 2020, **26**, 3364–3372.

19 (*a*) J. Pous, T. Courant, G. Bernadat, B. I. Iorga, F. Blanchard and G. Masson, *J. Am. Chem. Soc.*, 2015, **137**, 11950–11953; (*b*) N. Momiyama, H. Tabuse, H. Noda, M. Yamanaka, T. Fujinami, K. Yamanishi, A. Izumiseki, K. Funayama, F. Egawa, S. Okada, H. Adachi and M. Terada, *J. Am. Chem. Soc.*, 2016, **138**, 11353–11359; (*c*) T. Varlet, C. Gelis, P. Retailleau, G. Bernadat, L. Neuville and G. Masson, *Angew. Chem., Int. Ed.*, 2020, **59**, 8491–8496.

20 T. Nakanishi and M. Terada, *Chem. Sci.*, 2023, **14**, 5712–5721.

21 (*a*) A. D. Becke, *Phys. Rev. A*, 1988, **38**, 3098–3100; (*b*) C. Lee, W. Yang and R. G. Parr, *Phys. Rev. B*, 1988, **37**, 785–789.

22 (*a*) S. Grimme, J. Antony, S. Ehrlich and H. Krieg, *J. Chem. Phys.*, 2010, **132**, 154104; (*b*) S. Grimme, S. Ehrlich and L. Goerigk, *J. Comput. Chem.*, 2011, **32**, 1456–1465.

23 (*a*) S. Portela and I. Fernández, *J. Org. Chem.*, 2022, **87**, 9307–9315; (*b*) A. E. Davis, J. M. Lowe and M. K. Hilinski, *Chem. Sci.*, 2021, **12**, 15947–15952.

24 Chiral phosphoric acid catalysts: (*a*) N. Momiyama, H. Tabuse and M. Terada, *J. Am. Chem. Soc.*, 2009, **131**, 12882–12883; (*b*) Y.-Y. Wang, K. Kanomata, T. Korenaga and M. Terada, *Angew. Chem., Int. Ed.*, 2016, **55**, 927–931; (*c*) Y. Ota, A. Kondoh and M. Terada, *Angew. Chem., Int. Ed.*, 2018, **57**, 13917–13921; (*d*) S. Umemiya and M. Terada, *Org. Lett.*, 2021, **23**, 3767–3771; (*e*) T. Uchikura, N. Kamiyama, T. Mouri and T. Akiyama, *ACS Catal.*, 2022, **12**, 5209–5216; (*f*) T. Uchikura, K. Aruga, R. Suzuki and T. Akiyama, *Org. Lett.*, 2022, **24**, 4699–4703. For seminal studies of chiral phosphoric acid catalysts, see: (*g*) T. Akiyama, J. Itoh, K. Yokota and K. Fuchibe, *Angew. Chem., Int. Ed.*, 2004, **43**, 1566–1568; (*h*) D. Uraguchi and M. Terada, *J. Am. Chem. Soc.*, 2004, **126**, 5356–5357.

25 Y. Sudo, D. Shirasaki, S. Harada and A. Nishida, *J. Am. Chem. Soc.*, 2008, **130**, 12588–12589.